

Effect of breakup coupling on elastic scattering of the weakly bound projectile ${}^9\text{Be}$ from ${}^{89}\text{Y}$ target

C.S. Palshetkar¹, S. Santra¹, A. Chatterjee¹, A. Shrivastava¹, S.K. Pandit¹,
K. Ramachandran¹, V.V. Parkar², B.J.Roy¹, V. Jha¹, V. Nanal² and S. Kailas¹

¹Nuclear Physics Division, Bhabha Atomic Research Centre, Mumbai – 400 085, INDIA

²Department of Nuclear and Atomic Physics, Tata Institute of Fundamental Research, Mumbai – 400 085, INDIA

Introduction

Reaction studies with weakly bound nuclei over the last two decades have contributed significantly in understanding the effect of the structure of the projectile on its reaction mechanisms. Due to the low breakup threshold energies of these projectiles, the breakup channel is expected to be important in influencing other reaction channels. Particularly, in the case of scattering of the weakly bound stable projectiles, the influence of the breakup channel is seen in the energy dependence of the optical model (OM) potential around the Coulomb barrier. The real part of the potential does not show a prominent energy dependence while the imaginary part persist even below the barrier, unlike in the case of the tightly bound nuclei, an observation termed as breakup threshold anomaly (BTA). In the case of tightly bound nuclei, coupling to bound excited states produces an attractive real dynamic polarization potential (DPP) which becomes increasingly attractive as the projectile energy decreases to the Coulomb barrier. The imaginary part shows a decreasingly attractive trend in the same energy range thus leading to the observed threshold anomaly (TA). However, in case of weakly bound nuclei, the coupling to its continuum leads to a repulsive real DPP while the imaginary part becomes increasingly attractive, leading to the observed BTA. In the case of the ${}^6\text{Li}$ scattering from different targets, the BTA has been observed which has also been confirmed from the continuum discretized coupled-channels (CDCC) calculations. For ${}^7\text{Li}$, the conventional TA has been observed, whereas there are inconclusive or conflicting results for the case of ${}^9\text{Be}$ scattering. In the present contribution, the CDCC calculations performed for the ${}^9\text{Be}+{}^{89}\text{Y}$ system, with an aim to understand the energy dependence

of the OM potential obtained from the elastic scattering fit and the fusion cross section data [1], are presented.

Analysis

CDCC calculations have been performed for the ${}^9\text{Be}+{}^{89}\text{Y}$ system, using the experimental data in [2] and employing the code FRESKO [3] to understand the effect of continuum coupling of ${}^9\text{Be}$ states on its scattering. The cluster folding technique has been used with the ${}^4\text{He}+{}^5\text{He}$ cluster structure assumed for ${}^9\text{Be}$ and having breakup threshold energy of 2.467 MeV. The continuum with $L=0,1,2$ has been discretized into momentum bins from $k=0$ to 0.7 fm^{-1} with $\Delta k=0.15\text{ fm}^{-1}$ and the energies corresponding to each k have been assigned as the mean energy of the bins. Re-orientation couplings for ${}^9\text{Be}$ ground state have been included to take into account its large quadrupole deformation ($Q=+5.3\text{ e fm}^2$). The potential for binding the ${}^4\text{He}+{}^5\text{He}$ cluster has been taken from [4] with the depth of the potential been adjusted to reproduce the energy of each level. The ${}^4\text{He}+{}^{89}\text{Y}$ and ${}^5\text{He}+{}^{89}\text{Y}$ potentials have been taken to be of the Woods-Saxon form. The diffuseness of the latter has been increased by 0.1 fm to take into account its extended structure. Potential parameters for the ${}^4\text{He}+{}^{89}\text{Y}$ potential were obtained from OM fits to the experimental data for the system at 16 MeV [5] (which corresponds to $4/9$ times the ${}^9\text{Be}$ beam energy at 33.5 MeV - the highest energy in the current investigation). Along with the continuum, couplings to the $5/2^-$ state ($E_x=2.429\text{ MeV}$) and the $7/2^-$ resonant state ($E_x=6.38\text{ MeV}$) in ${}^9\text{Be}$ have been included considering them as $L=2$ states. The $7/2^-$ state has been taken as a continuum state with width of 3 MeV , while the $5/2^-$ state is taken as a bound state due to ${}^4\text{He}+{}^5\text{He}$ structure considered for ${}^9\text{Be}$. Results

from the CDCC calculations thus obtained have been plotted in Fig. 1 by the solid line while the uncoupled calculations have been represented by dot-dash line.

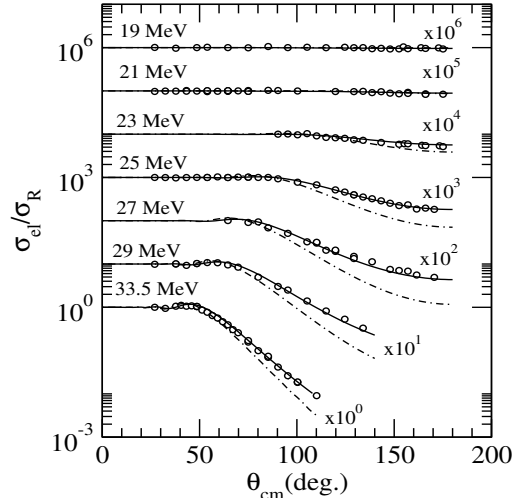


Fig. 1 Ratio of the elastic to Rutherford cross-sections for the $^9\text{Be}+^{89}\text{Y}$ system along with results of uncoupled (dot-dash) and CDCC (solid) calculations.

In Fig. 2, comparison of the experimental CF (triangles) and total fusion (TF=CF+ICF) cross-sections (diamonds) for the system [1] with the absorption cross-sections obtained after continuum coupling (dashed line) and the BPM calculations (solid line) has been done.

Discussion

Results for the elastic scattering cross-sections obtained from continuum coupling (solid lines), were found to reproduce the experimental values well, as shown in Fig. 1. Interestingly, at backward angles, the values were found to be enhanced as compared to the uncoupled results (dot-dash lines). This suggests that the real DPP generated due to breakup coupling is repulsive. This is consistent with the observed energy dependence of the OM potential for $^9\text{Be}+^{89}\text{Y}$ [2] where the real part has no pronounced bump around the Coulomb barrier and the associated imaginary part remains non-zero at sub-barrier energies. In Fig. 2, the reaction cross-sections obtained from CDCC calculations, cumulative absorption by imaginary potential and fusion by BPM are compared with the experimental fusion

[1] and the reaction cross-sections obtained by OM fit. The calculated reaction cross-sections (dotted line) reproduce the reaction cross-sections obtained from OM analysis (filled circles) very well. The BPM fusion (solid line) at energies above the barrier overestimates both CF as well as TF though they were expected [6] to reproduce the experimental TF. This can be due to the fact that only a lower limit of ICF cross-sections was measured experimentally due to the long half-life ($\sim 3 \times 10^7$ yrs) of the evaporation residue corresponding to the ICF channel. The cumulative absorption cross-sections (dashed line) were found to over-estimate the TF cross-sections, a result similar to that found in [6]. This suggests that the excess of absorption cross-sections from calculations may be attributed to the uncoupled transfer and target inelastic channels. If all the channels were coupled together then the absorption cross-sections would be equal to TF.

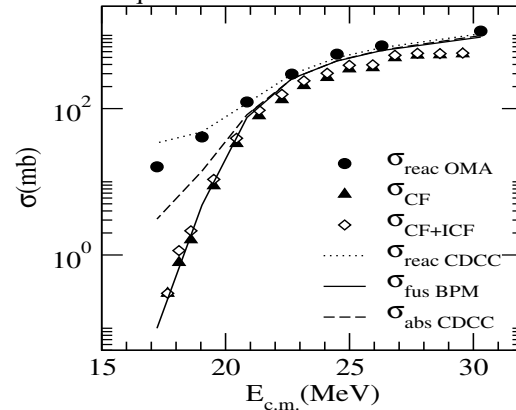


Fig. 2 Comparison of the experimental CF and TF cross-sections with the theoretical estimates for the same from CDCC calculations.

References

- [1] C.S. Palshetkar et al., Phys. Rev. C **82**, 044608 (2010)
- [2] C.S. Palshetkar et al., DAE Symp. On. Nucl. Phys. **B33**, 427 (2008)
- [3] I.J. Thompson, version FRES2.8
- [4] N. Keeley et al., Phys. Rev. C **64**, 031602(R) (2001)
- [5] G.G. Kiss et al., Phys. Rev. C **80**, 045807 (2009)
- [6] S.Santra et al., Phys. Rev. C **83**, 034616 (2011)